magnesium nitrate, the phonon mean free path can
be at least as long as 3.5 mm. Further support
of this conclusion is given by recent heat-pulse-
propagation experiments which clearly show bal-
listic-phonon propagation across 5-mm samples.
This work will be described elsewhere.

[1]W. R. Abel, A. C. Anderson, W. C. Black, and J. C. Wheatley, Phys. Rev. Lett. **16**, 273 (1966).

[2]W. C. Black, A. C. Mota, J. C. Wheatley, J. H. Bishop, and P. M. Brewster, J. Low Temp. Phys. **4**, 391 (1971); M. P. Bertinat, D. F. Brewer, and J. P. Harrison, J. Low Temp. Phys. **2**, 157 (1970).

[3]A. J. Leggett and M. Vuorio, J. Low Temp. Phys. **3**, 359 (1970).

[4]J. E. Robichaux and A. C. Anderson, Phys. Rev. B **2**, 5035 (1970).

[5]J. N. Haasbroek, in International Conference on Phonon Scattering in Solids, Paris, 1972 (unpublished).

[6]R. A. Fisher, Rev. Sci. Instrum. **43**, 386 (1972).

[7]R. O. Pohl, Phys. Rev. **118**, 1499 (1960).

[8]P. D. Thacher, Phys. Rev. **156**, 975 (1967).

[9]See, for instance, M. V. Klein, and R. F. Caldwell, Rev. Sci. Instrum. **37**, 1291 (1966).

[10]W. D. Seward, Ph.D. thesis (Cornell University, 1965) (unpublished); Materials Science Center Report No. 368 (unpublished).

[11]H. B. G. Casimir, Physica (The Hague) **5**, 495 (1938). Note that on p. 497 of this paper, the second equation should contain $8\pi/3$ instead of $4\pi^2/3$. See also P. Carruthers, Rev. Mod. Phys. **33**, 92 (1961).

[12]S. L. McBride (private communication).

[13]C. A. Bailey, Proc. Phys. Soc. Lond. **83**, 369 (1964).

[14]The method of measurement is described by T. H. Chou, S. L. McBride, and N. Rumin, Can. J. Phys. **49**, 1597 (1971).

Lattice Dynamics of Ionic Microcrystals

T. P. Martin

Max Planck Institut für Festkörperforschung, 7 Stuttgart, Germany

(Received 25 October 1972)

The density of phonon states and infrared absorption of RbF microcrystals have been calculated using a rigid-ion model. The microcrystals were assumed to be rectangular solids containing up to 144 atoms. The density of states of the microcrystals, although shifted to lower frequency, was found to have the same shape as the density of states assuming cyclic boundary conditions. The fundamental infrared absorption could be characterized as three distinct bands due to edge modes, surface modes, and volume modes. These absorption bands split in crystals with noncubic shape, in surprisingly good agreement with a continuum theory. In addition to the fundamental absorption, the calculation displayed a weak low-frequency absorption which resembled the density of states.

I. INTRODUCTION

Considerable attention has been given to the macroscopic phonon properties of finite crystals.[1] An important macroscopic effect in small polar crystals is a shift in the optically active modes of vibration due to surface polarization. This macro-scopic effect can be calculated using a continuum model of the crystal, i.e., by applying the ap-propriate electromagnetic boundary conditions to a material described by a frequency-dependent complex dielectric function. With the inclusion of retardation, the continuum model can be applied to crystals of arbitrary size. Polariton modes localized at a plane surface have been predicted by this model[2,3] and have been observed experi-mentally.[4,5] Although many surface effects have been successfully explained by the continuum model, it has distinct limitations. The model

contains only one characteristic frequency, the pole of the dielectric function, which describes the crystal. Clearly, such a model cannot be expected to describe effects which are dependent on the structure of the phonon density of states. In addi-tion, the continuum model cannot be used for modes so highly localized that the crystal's atomicity is important.

Less attention has been given to the microscopic phonon properties of a finite crystal, that is, those properties that depend on the perturbed na-ture of the atomic layers at the surface. One reason for this lack of attention is that the contin-uum model is not appropriate to predict micro-scopic effects. An alternative approach, which is appropriate, is a lattice-dynamical calculation which considers the finite crystal to be a large molecule. Such a calculation has the advantage that it contains a microscopic description of the

surface; however, it has the disadvantage that one must ultimately diagonalize very large matrices. Lucas[6] and Tong and Maradudin[7] have made a lattice-dynamical study of the modes of vibration of an ionic slab containing a small number of atomic layers. Allen, Alldredge, and de Wette[8-10] have made a more extensive study of semi-infinite crystals. They have used models including long-range Coulomb interactions, ion deformations, and relaxation of surface atoms. The most important result of these calculations is that modes of vibration localized to within a few atomic layers of the surface should be observable. One way to observe this new type of surface mode is to devise an experiment which is sensitive to the motion of a relatively small number of atoms at a single surface. In fact, such an experiment appears to have been performed by Ibach,[11] who has scattered low-energy electrons from a silicon surface. Since only the surface silicon atoms have an appreciable effective charge, the observed surface phonon must be highly localized.

An alternative method to observe microscopic surface modes would be to prepare samples with a large surface-to-volume ratio. This is most easily done, not with slabs, but with small particles. Powder samples could be used in more conventional experiments such as infrared absorption, Raman scattering, neutron scattering, and x-ray scattering. Rieder and Hörl,[12] in fact, have made neutron scattering measurements on 100-Å MgO crystals.

Anticipating further experiments on powder samples, we present here the calculated density of states and infrared absorption of polar microcrystals. Preliminary work[13] in this direction has left many questions unanswered because no attempt was made to distinguish bulk effects from surface effects. In this work, we have made a more complete study using parameters appropriate for RbF. Kellermann's[14] rigid-ion model has been used. The simplicity of this model is perhaps appropriate, considering the lack of experimental data. RbF has been chosen for several reasons. Rieder[15] has proposed the study of surface modes within a density-of-states gap using neutron scattering techniques. RbF has a well-defined gap. In addition, Chen, Alldredge, and de Wette[16] have already made lattice-dynamical calculations for a RbF slab. Although we have chosen to present results for RbF, calculations have been made using parameters appropriate for other ionic crystals as well. The qualitative results and conclusions of this work seem to be general for all ionic microcrystals.

II. CALCULATION

According to the method of Kellermann,[14] the force-constant matrix $\underline{\Phi}$ used in the equation of motion for normal mode p,

$$\underline{M}^{-1/2}\,\underline{\Phi}\,\underline{M}^{-1/2}\,\vec{X}_p = \omega_p\,\underline{I}\,\vec{X}_p\,, \tag{1}$$

is separated into a long-range Coulomb-interaction term, $\underline{\Phi}_C$, and a short-range term, $\underline{\Phi}_r$. An element of $\underline{\Phi}_C$ can be written

$$\Phi_C(l\kappa\alpha,\ l'\kappa'\alpha') = \frac{E_\kappa E_{\kappa'}}{|\vec{r}(l\kappa,\ l'\kappa')|^3}$$

$$\times\left(-\delta_{\alpha\alpha'} + \frac{3r_\alpha(l\kappa,\ l'\kappa')\,r_{\alpha'}(l\kappa,\ l'\kappa')}{|\vec{r}(l\kappa,\ l'\kappa')|^2}\right)\,, \tag{2}$$

where E_κ is the effective charge of ion κ and $\vec{r}(l\kappa, l'\kappa')$ is the vector between the equilibrium position of atom $l\kappa$ and atom $l'\kappa'$. The elements of $\underline{\Phi}_r$ are assumed to be zero unless they connect nearest neighbors. If the magnitude of the vector between nearest neighbors is written r_0, then a nonzero element of $\underline{\Phi}_r$ can be written

$$\Phi_r(l\kappa\alpha,\ l'\kappa'\alpha') = \frac{E_\kappa E_{\kappa'}}{4r_0^3}$$

$$\times\left(B\delta_{\alpha\alpha'} + \frac{(A-B)r_\alpha(l\kappa,\ l'\kappa')r_{\alpha'}(l\kappa,\ l'\kappa')}{r_0^2}\right)\,. \tag{3}$$

We have assumed that the mass matrix $\underline{M}$ used in Eq. (1) is defined by

$$M(l\kappa\alpha,\ l'\kappa'\alpha') = \delta_{ll'}\,\delta_{\kappa\kappa'}\,\delta_{\alpha\alpha'}\,M_\kappa^{-1/2}\,,$$

where M_κ is the mass of ion κ. The distance between nearest neighbors in the microcrystal is assumed to be that of the bulk material. This leaves three parameters to be specified; A, B, and $E_\pm$. Using the condition of lattice stability, E_+ can be related to B through the Madelung constant. For NaCl structure the relation is

$$B = 1.165(E_\pm/e)^2\,. \tag{4}$$

The remaining two independent model parameters can be expressed in terms of the reststrahl frequency ω_T and compressibility K:

$$\left(\frac{E_\pm}{e}\right)^2 = \frac{9r_0^4}{\pi K e^2} - \frac{3\omega_T^2\mu r_0^3}{2\pi e^2}\,, \tag{5}$$

$$A = 12r_0^4/Ke^2 - 2B\,. \tag{6}$$

The reduced mass of the unit cell has been denoted by μ. Using Eqs. (4)–(6) and the appropriate values of r_0, ω_T, and K, the model parameters for RbF are found to be

$$A = 10.197\,,\quad B = -1.029\,,\quad E_+ = -E_- = 0.94e\,. \tag{7}$$

The problem of the lattice dynamics of a microcrystal can be formulated very simply: Eq. (1). There remains, however, the considerable computational problem of finding the eigenvectors and eigenvalues of a very large dynamical matrix. The size and speed of the computer available will determine how large a crystal can be considered. For example, we have available a CDC 6600 com-

puter with a total core memory of about 130 000 words. However, the core conveniently available to the programer is only 60 000 words. A cube composed of 216 ions, i.e., six ions on an edge, requires 417 516 words merely to define the dynamical matrix. Additional core is required for the eigenvectors and intermediate transformation matrices. Clearly, the problem must be solved "out of core." Renolds[17] has developed such a program using Householder's method[18] to tridiagonalize the matrix and Rutishauser's symmetric $L-R$ method[19] to obtain the eigenvalues.

Once the eigenvectors and eigenvalues are known, it is possible to calculate an absorption coefficient defined by

$$\alpha(\omega) = \frac{2\pi^2 N}{3cn(\omega)} \sum_{l\kappa\alpha} \sum_{l'\kappa'\alpha'} E_\kappa E_{\kappa'} (M_\kappa M_{\kappa'})^{-1/2}$$

$$\times \sum_{p} X_p(l\kappa\alpha) X_p(l'\kappa'\alpha')\delta(\omega_p, \omega), \quad (8)$$

where N is the number of crystals per unit volume, c is the velocity of light, $n(\omega)$ is the real part of the index of refraction at frequency ω, and E_κ and M_κ are the effective charge and the mass of atom κ. For a low density powder $n(\omega)$ can be set equal to 1. No local-field correction has been used in Eq. (8). The local field will in fact be different for different ions. However, we feel that the use of a realistic local field is not necessary, or perhaps even desirable, if the result of the calculation is to be compared with experiments on much larger crystals.

One cannot easily display all the eigenvectors of a microcrystal. A list of 417 516 eigenvector components would be impossible to analyze. It is more useful to use the eigenvectors to generate functions that demonstrate, for example, at which frequency surface modes are important. Such a function is the so-called projected density of states, defined in the case of a surface by the expression

$$F_s(\omega) = \sum_{\substack{l\kappa \\ \text{surface}}} \sum_p |X_p(l\kappa)|^2 \delta(\omega_p, \omega). \quad (9)$$

The first summation is to be carried out over only surface atoms. This function shows the frequency interval in which the surface atoms (or the edge atoms, or the corner atoms) have large displacements for a large number of modes.

III. RESULTS AND DISCUSSION

A. Density of States

The dashed histogram in Fig. 1 shows the density of states of RbF, assuming cyclic boundary conditions. A sampling of 1000 points in the Brillouin zone was made. There is a gap in the density of states between 2.25 and 2.75×10¹³ rad/
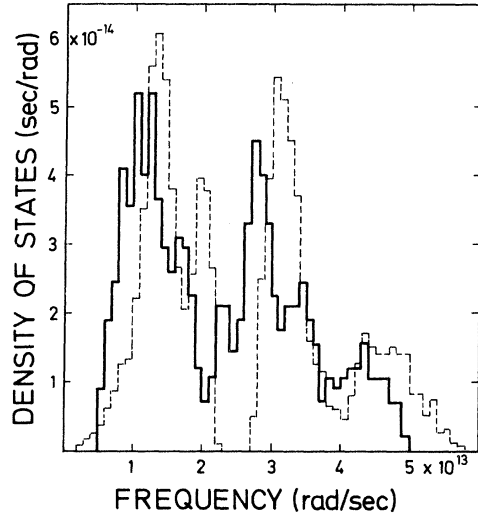

FIG. 1. Calculated rigid-ion density of states of a RbF cube containing 64 atoms (solid line) and RbF using cyclic boundary conditions (dashed line).

sec, separating the acoustical and optical modes. In addition, there are four distinct peaks in the density of states corresponding to critical points at the Brillouin-zone edge. In order to smooth out the histograms, we have assumed that a mode of vibration contributed not only to the frequency interval in which its eigenfrequency falls but also to one frequency interval on each side.

We have used the same rigid-ion parameters to calculate the density of states of a microcrystal containing only 64 atoms. Clearly, this approximation is invalid for such small microcrystals. The bulk parameters are used merely because of the large amount of computer time that would be necessary to calculate more appropriate parameters. However, it is possible to partially justify the approximation. We would like to compare our results with experiments on crystals containing millions of atoms. If, in this calculation, the surface ions were allowed to relax, the effects would be so exaggerated as to make such a comparison difficult.

The solid histogram in Fig. 1 shows the density of states of a RbF microcrystal with cubic shape and with four atoms on an edge. This histogram is quite similar to the density-of-states histogram of the bulk material. The four peaks previously mentioned show clearly in the density of states of the microcrystal. This similarity is surprising but not implausible. The peaks in the density of states, assuming cyclic boundary conditions, correspond to short-wavelength modes. It is just these short-wavelength modes that should be best reproduced in a microcrystal. The low-frequency long-wavelength modes are absent in the micro-

crystal.

The principal effect of the surface seems to be to shift the entire density-of-states curve of the microcrystal to lower frequency. This effect too can be made plausible if one remembers that the restoring force on atoms at the surface is reduced, and that 56 of the 64 atoms in this microcrystal are on the surface.

No gap exists in the density of states of the microcrystal. In fact, Fig. 1 shows a peak within the gap at 2.3×10^{13} rad/sec. In order to determine whether this peak is experimentally observable in larger crystals, we must examine the modes contributing to the peak in more detail. Figure 2 shows the density of states projected onto the surface atoms, onto the edge atoms, and onto the corner atoms. Clearly, the modes contributing to the gap peak may be characterized as corner modes. Therefore, this peak may be expected to become less important as the microcrystal becomes larger. That this is indeed the case is shown in Fig. 3. The solid histogram in Fig. 3 represents the density of states of a RbF crystal six atoms long, six atoms high, and four atoms wide. The peak within the gap has disappeared for this larger microcrystal.

A comparison of Figs. 2 and 3 shows that the density of states of a microcrystal approaches the density of states of an infinite crystal as the microcrystal becomes larger. In particular, the rela-
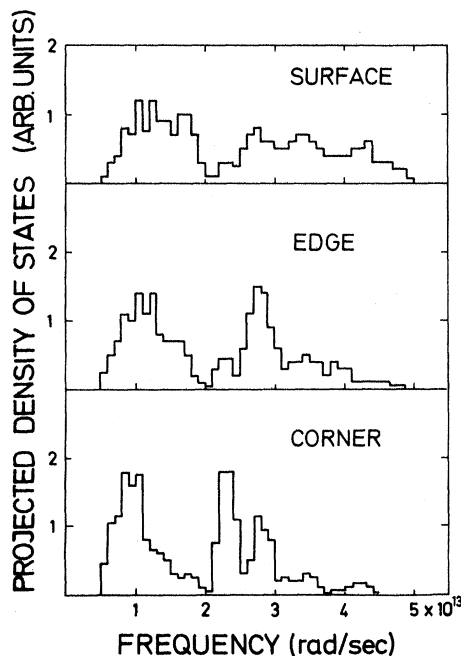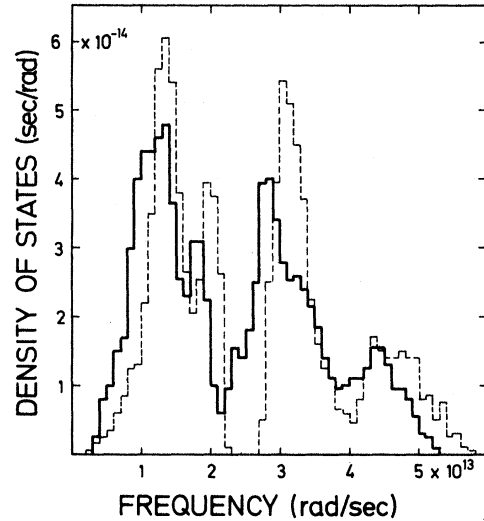

FIG. 3. Calculated rigid-ion density of states of a RbF microcrystal with atomic dimensions $4 \times 6 \times 6$ (solid line) and RbF using cyclic boundary conditions (dashed line).

tive displacement of the two histograms is smaller in Fig. 3 due to the smaller percentage of surface atoms in the microcrystal. This reassuring trend convinced us that it is not necessary to consider even larger microcrystals.

It is useful to represent relatively small changes in the density of states by plotting a difference spectrum, i. e., the density of states of the microcrystal minus the density of states assuming cyclic boundary conditions. This spectrum is particularly interesting since Chen et al.[16] have calculated a similar function for a semi-infinite RbF crystal. The two spectra are compared in Fig. 4. Despite the fact that Chen et al.[16] used an 11-parameter breathing-shell model, the two spectra are quite similar.

It is tempting to interpret a peak in a difference spectrum as an indication of surface modes. The result of this calculation shows that for microcrystals such an interpretation is dangerous. It seems more likely that the difference spectrum illustrates a frequency displacement of the density of states of microcrystals, i. e., $g(\omega) - g(\omega + \Delta\omega)$. Therefore, a peak in the difference spectrum is associated with every large positive slope in the density of states.

B. Absorption

In the harmonic approximation, an alkali halide crystal with translational symmetry absorbs light only at the frequency of the long-wavelength transverse-optical mode of vibration ω_T. If the translational symmetry is destroyed by making one or more dimensions of the crystal finite, the low-

FIG. 2. Density of states projected onto the surface atoms, the edge atoms, and the corner atoms of a RbF cube containing 64 atoms.
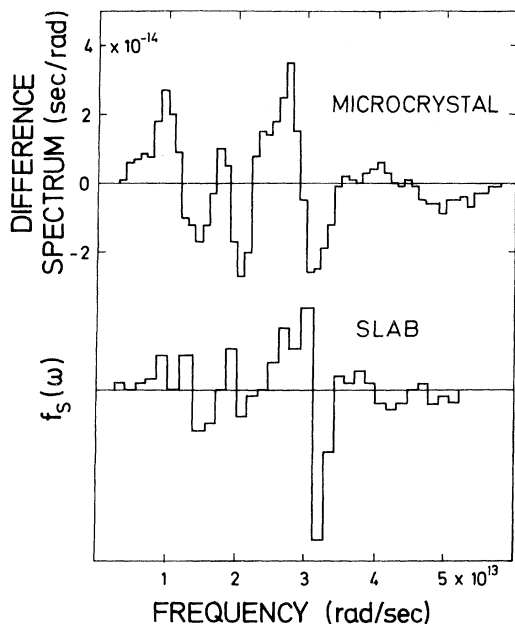
FIG. 4. Calculated difference spectrum obtained by subtracting the density of states of RbF with cyclic boundary conditions from the density of states of a $4 \times 6 \times 6$ microcrystal (top curve) and the difference spectrum for a slab containing 15 layers [bottom curve, from Chen, Alldredge, and de Wette (Ref. 16)].

frequency acoustical modes acquire a dipole moment. A weak surface-induced acoustical-mode absorption will result. In addition, the fundamental absorption of small crystals is shifted from ω_T to higher frequencies by the surface depolarization. It is not obvious that the absorption of extremely small microcrystals can be classified into these two types, i.e., into (i) surface-induced acoustical-mode absorption and (ii) fundamental polariton absorption. The first classification assumes the surface to be a perturbation on the crystal and the second classification assumes a continuum model of the crystal. Clearly, neither assumption holds for crystals containing, for example, 64 atoms. In the case of a microcrystal, one might expect a limited number of optically active molecular vibrations with varying oscillator strengths. Perhaps one of the most interesting results of this calculation is that the absorption of microcrystals does indeed separate into surface-induced acoustical-mode absorption and fundamental polariton absorption.

1. Fundamental Absorption

If a spherical polar crystal is small compared to the wavelength of light at ω_T but still large compared to atomic dimensions, then the fundamental absorption should occur at the Fröhlich frequency normally defined as[20]

$$\omega_s^2 = \frac{\epsilon_0 + 2}{\epsilon_\infty + 2} \, \omega_T^2 , \tag{10}$$

where ϵ_0 and ϵ_∞ are the low- and high-frequency dielectric constants, respectively. A frequency defined in this manner is not appropriate for comparison with this rigid-ion calculation unless two modifications are made. Since we have assumed that the crystal has no electronic polarizability, ϵ_∞ should, for consistency, be set equal to 1. In addition, the microscopic parameter ϵ_0 does not enter into the determination of the rigid-ion model parameters used in this calculation. Therefore, it would be more appropriate to calculate ϵ_0 from the value of ω_L resulting from the model calculation and from the Lyddane–Sachs–Teller relation, i.e.,

$$\epsilon_0 = \omega_L^2 / \omega_T^2 . \tag{11}$$

With these two modifications Eq. (10) becomes

$$\omega_s^2 = \tfrac{1}{3}(\omega_L^2 + 2\omega_T^2) . \tag{12}$$

The calculated absorption coefficient of a powder sample composed of 64-atom microcrystals is shown in Fig. 5. Notice that this curve resembles neither the density of states nor the single-peak absorption of a large crystal. The strongest absorption can be seen to occur in the form of three distinct peaks between ω_T and ω_L.

Of the 192 modes of vibration of a 64-atom microcrystal only five triply degenerate modes have a large dipole moment. An examination of the
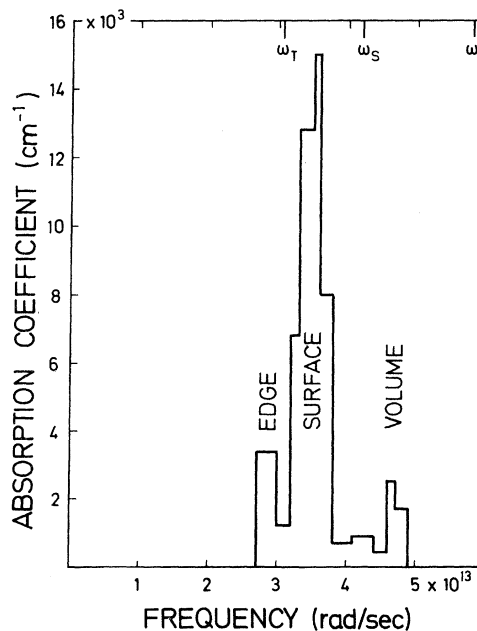

FIG. 5. Calculated infrared-absorption coefficient of a powder sample composed of RbF microcrystals, each containing 64 atoms.

eigenvectors of these 15 modes shows that the three absorption peaks can be characterized as either edge-, surface-, or volume-mode absorption, as shown in Fig. 5. Such a characterization is not apparent by examining the projected density of states shown in Fig. 2, because the 15 highly absorbing modes play no special role in defining these functions. All modes of vibration contribute to the projected density-of-states functions.

The fact that the fundamental absorption of the microcrystal occurs between ω_T and ω_L is in agreement with the continuum theory. However, the peak absorption does not occur at ω_s, the frequency at which the continuum theory predicts a mode with uniform polarization. This mode, which plays such an important role in continuum theory, is not found in these calculations. That is, none of the 15 eigenvectors corresponds to a uniform motion of all the positive ions against all the negative ions. However, one cannot conclude that our result is inconsistent with continuum theory. The mode with uniform polarization is expected, even in the continuum theory, only for an ellipsoid. The microcrystals in our calculation have a cubic shape. The continuum model has not yet been applied to a cube, although recent work on a dielectric wedge[21] is a step in this direction.

The absorption coefficient calculated for a powder sample composed of microcrystals containing 144 atoms is shown in Fig. 6. These microcrystals have atomic dimensions $4 \times 6 \times 6$. Comparing Figs. 5 and 6, we see that for the 144-atom microcrystal, the edge-mode absorption decreases, the surface-mode absorption increases, and the volume-mode absorption increases. This observation can be explained by the different percentage of edge, surface, and volume atoms in the two microcrystals, as indicated in Table I.

In addition to this relative change in the peak heights, the main absorption peak is clearly split for the $4 \times 6 \times 6$ microcrystal (Fig. 6). Such a splitting is not unexpected in a rectangular solid. A triply degenerate "surface mode" should split into a double-degenerate low-frequency mode and a nondegenerate high-frequency mode. The splitting is even predicted by the continuum theory. Although the continuum theory cannot be applied to a rectangular solid, for a general ellipsoid Eq. (12) becomes
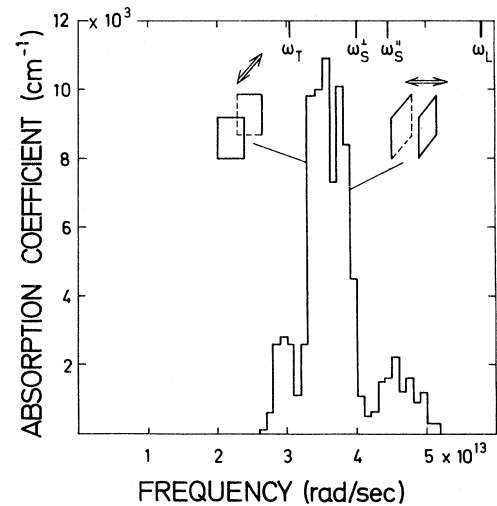

FIG. 6. Calculated infrared-absorption coefficient of a powder sample composed of RbF microcrystals, each with atomic dimensions $4 \times 6 \times 6$.

$$\omega_j^2 = g_j \omega_L^2 + (1 - g_j)\omega_T^2 , \qquad (13)$$

where g_j is one of the three shape factors appropriate for the ellipsoid. An ellipsoid whose principal axes have the ratio $4 : 6 : 6$ would have its infrared absorption at the frequencies indicated by $\omega_s^\perp$ and $\omega_s^\parallel$ in Fig. 6. It is apparent that the splitting and polarization expected from continuum theory is the same as that obtained from the lattice-dynamical calculation.

2. Surface-Induced Acoustical-Mode Absorption

In addition to the few strongly absorbing modes between ω_T and ω_L, there are many weakly absorbing modes at lower frequencies. Figure 7 shows the surface-induced acoustical-mode absorption of RbF microcrystals containing 144 atoms. The sample is assumed to be composed of randomly oriented crystals and to have the same density as bulk RbF. A comparison of Figs. 3 and 7 shows that the two low-frequency absorption peaks correspond to peaks in the density of states. There exists an additional absorption peak within the gap. This peak is due to corner-atom absorption and can be expected to disappear for larger microcrystals.

TABLE I. Composition of microcrystals.

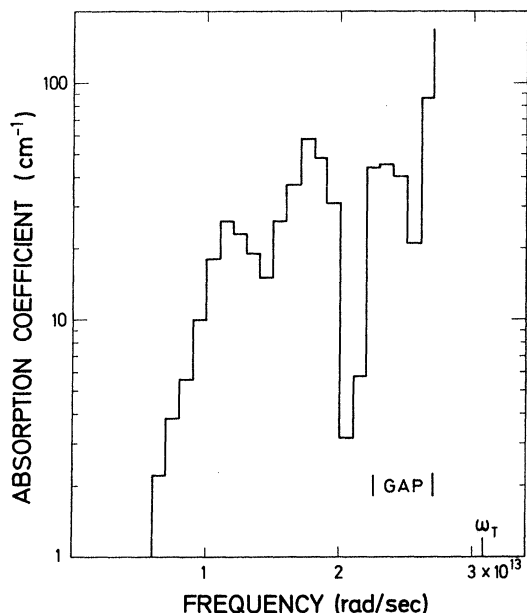| Microcrystal size	Corner atoms (%)	Edge atoms (%)	Surface atoms (%)	Volume atoms (%)
$4 \times 4 \times 4$	12.5	37.5	37.5	12.5
$4 \times 6 \times 6$	5.5	27.8	44.4	22.2

FIG. 7. Low-frequency infrared-absorption coefficient of a powder sample composed of RbF microcrystals, each with atomic dimensions $4 \times 6 \times 6$.

An experiment to observe the surface-induced absorption would be difficult. The experiment must be performed at low temperature to reduce two-phonon absorption. A thick sample must be used since the surface-induced absorption is expected to be very weak. Even a small scattering cross section in such a sample would be troublesome. Scattering from the particles themselves, from the voids between the particles, and from clumps of particles will always be present. Pressing the powder sample will tend to make it more homogeneous and therefore less subject to scattering. The particles in a pressed powder will strong-ly interact; but this interaction will not destroy the effect, which depends basically on the lack of translational symmetry. In addition, a twofold advantage could be gained from using extremely small (10–100 Å) particles. The scattering from individual particles would be minimized and the surface-induced absorption would be enhanced to a convenient level.

IV. CONCLUSION

The shape of the density of states of microcrystals containing only 64 and 144 atoms is very similar to the density of states of a crystal assuming cyclic boundary conditions. However, the entire curve for microcrystals is shifted to lower frequencies. This shifted density of states is just that calculated for a 15-layer slab, leading one to the tentative conclusion that density-of-states effects in finite crystals will be essentially geometry independent. The eigenvectors of the individual modes will, of course, be quite different for microcrystals and slabs. The infrared absorption of microcrystals can be characterized as strong fundamental absorption occurring between ω_T and ω_L and weak surface-induced acoustical-mode absorption. The fundamental absorption displays three peaks, which can be conveniently characterized as absorption by a small number of edge, surface, and volume modes, respectively. The surface-induced acoustical-mode absorption displays the density-of-states structure.

ACKNOWLEDGMENTS

[1] For a recent review see, R. Ruppin and R. Englman, Rep. Prog. Phys. 33, 149 (1970).
[2] K. L. Kliewer and R. Fuchs, Phys. Rev. 144, 495 (1966).
[3] R. Ruppin, Solid State Commun. 8, 1129 (1970).
[4] N. Marschall and B. Fischer, Phys. Rev. Lett. 28, 811 (1972).
[5] V. V. Bryksin, Y. M. Gerbstein, and D. N. Mirlin, Fiz. Tverd. Tela 13, 2125 (1971) [Sov. Phys.-Solid State 13, 1779 (1972)].
[6] A. A. Lucas, J. Chem. Phys. 48, 3156 (1968).
[7] S. Y. Tong and A. A. Maradudin, Phys. Rev. 181, 1318 (1969).
[8] R. E. Allen, G. P. Alldredge, and F. W. de Wette, Phys. Rev. B 4, 1648 (1971).
[9] R. E. Allen, G. P. Alldredge, and F. W. de Wette, Phys. Rev. B 4, 1661 (1971).
[10] G. P. Alldredge, R. E. Allen, and F. W. de Wette, Phys. Rev. B 4, 1682 (1971).
[11] H. Ibach, Phys. Rev. Lett. 27, 253 (1971).

[12] K. H. Rieder and E. M. Hörl, Phys. Rev. Lett. 20, 209 (1968).
[13] L. Genzel and T. P. Martin, Phys. Status Solidi B 51, 101 (1972).
[14] E. W. Kellermann, Philos. Trans. R. Soc. Lond. 238, 513 (1940).
[15] K. H. Rieder (private communication).
[16] T. S. Chen, G. P. Alldredge, and F. W. de Wette, Solid State Commun. 10, 941 (1972).
[17] R. R. Renolds (private communication).
[18] See, for example, J. H. Wilkinson, The Algebraic Eigenvalue Problem (Clarendon, Oxford, 1965).
[19] H. Rutishauser and H. R. Schwarz, Numer. Math. 5, 273 (1963).
[20] H. Fröhlich, Theory of Dielectrics (Clarendon, Oxford, 1949).
[21] L. Dobrzynski and A. A. Maradudin, Phys. Rev. B 7, 1207 (1973).